Transactions, SMiRT-23
Manchester, United Kingdom - August 10-14, 2015
Division VI, Paper ID 426

SUMMARY OF THE BEHAVIOR OF STEEL-PLATE COMPOSITE (SC) WALLS SUBJECTED TO IMPULSIVE LOADS

Jakob C. Bruhl, P.E.[1] and Amit H. Varma, Ph.D.[2]

[1] Ph.D. Candidate, Purdue University, West Lafayette, IN, USA; Lieutenant Colonel, United States Army
[2] Professor, Lyles School of Civil Engineering, Purdue University, West Lafayette, IN, USA

ABSTRACT

Steel-plate composite (SC) walls are a viable alternative to reinforced concrete (RC) for protective structures and offer several advantages over RC. Current blast resistant design standards describe methods to design protective structures using RC, structural steel, or masonry in part because of the available experimental database for these materials to validate design methods. While there are blast test results of steel-concrete composite panels available in the literature, they are few and the majority are of specific configurations making it difficult to extrapolate to general behavior. This paper reports representative experimental results of simply supported one-way steel-plate composite (SC) wall sections, designed in accordance with AISC N690s1 Appendix N9 (AISC, 2014), and loaded with short duration uniform pressure pulses representative of far-field blast effects. Two numerical methods to assess the performance of SC walls subjected to blast loads are discussed and comparisons of experimental to numerical results are provided.

INTRODUCTION

Steel-plate composite (SC) walls consist of two steel faceplates and a plain concrete infill as shown in Figure 1. The faceplates provide flexural reinforcement and also serve as formwork. Composite action is provided by steel headed stud anchors on both faceplates. Positioning the faceplates at the extreme fiber of the cross-section maximizes their influence on flexural resistance and tension reinforcement is provided in all planer directions (Varma et al., 2014). Because the faceplates serve as formwork the need for temporary formwork structures is eliminated which reduces construction time. Transverse shear reinforcement is provided by steel bars, structural steel sections, or rectangular plates.

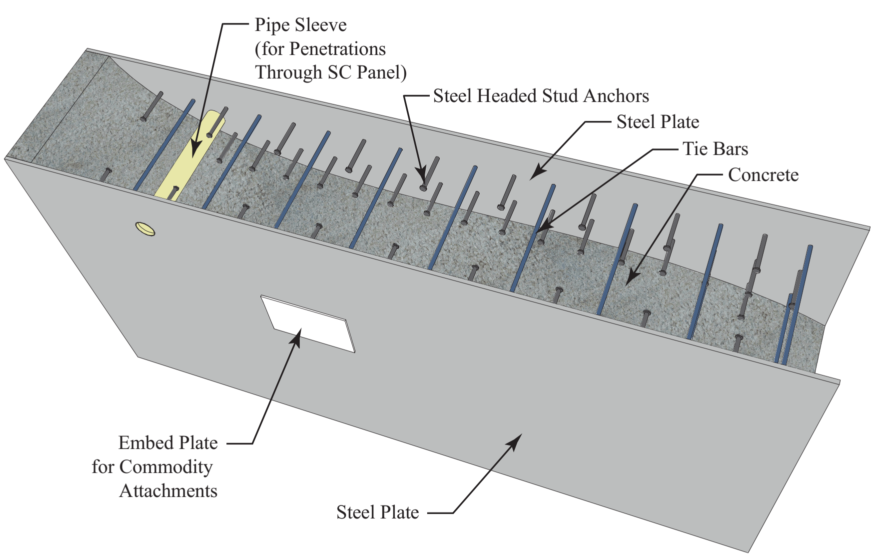

Figure 1. Typical SC Wall Section (from Johnson et al. (2014))

Reinforced concrete (RC) has historically been the preferred choice for blast resistant structures. SC walls are a viable alternative and offer several advantages over RC: (i) steel plates on the outside of the concrete maximize flexural resistance of the section, (ii) the plates serve as formwork which reduces construction time, and (iii) SC modules can be prefabricated which improves construction efficiency. Similar to RC, SC structures combine tensile strength and ductility of steel with compressive strength of concrete.

A specification for the design of SC walls for flexure, in-plane shear, and out-of-plane shear has recently been published as Appendix N9 of AISC N690s1 (AISC, 2014), a supplement to AISC N690-12 (AISC, 2012). Methods to design SC structures to resist the local effect of impacts, such as from an aircraft or tornado or hurricane-borne projectile, have been experimentally validated (Bruhl et al., 2015b; Grisaro & Dancygier, 2014). Quantifying the total and global response of SC structures subjected to impact loads can be accomplished using dynamic analysis methods such as single-degree-of-freedom (SDOF) models or a two-degree-of-freedom (TDOF) model which accounts for both the local and global contributions to total response (Bruhl et al., 2015a; Bruhl et al., 2015c).

Steel-concrete composite panels of various configurations have been subjected to blast loads (Heng et al., 1995; Hulton & Gough, 1999; Hulton, 1995; Lan et al., 2005; Liew & Wang, 2011). With the exception of methods to design Bi-Steel™ walls (Coyle and Cormie 2009), no blast resistant design guidance for SC walls has been developed. This paper describes the behavior of simply supported one-way SC wall sections subjected to short-duration pressure pulses. These pulses were generated by a blast load simulator (BLS) operated by the US Army Corps of Engineers, Engineering Research and Development Center (USACE-ERDC) in Vicksburg, MS. The pressure was approximately uniform across the face of the specimens, simulating far-field blast effects. Time histories of displacement at two locations, mid-span acceleration, faceplate strains, and pressure were recorded for each specimen.

Two numerical modelling methods were benchmarked to these experimental results: (1) a lumped mass, single-degree-of-freedom (SDOF) model using an experimentally developed static resistance function, and (2) a detailed non-linear finite element (FE) model analyzed using the commercial software LS-DYNA. These benchmarked models can be used to better understand the influence of design and loading parameters making them particularly useful in analysis of existing or new SC structures.

BACKGROUND

Blast tests of various configurations of steel-composite panels have been conducted by other researchers. Heng et al. (1995) described results from near-field blast tests of one-third scale fully enclosed steel-concrete-steel (SCS) sandwich panels. Their panel design contained no internal components (shear studs or tie bars) and the concrete core was enclosed by steel plates on all sides. Lan et al. (2005) described results from a series of blast tests of three different panel types: (i) steel fiber reinforced concrete (SFRC), (ii) profiled steel sheeting reinforced concrete (PSSRC), and (iii) SCS panels similar to those by Heng et al. (1995). Tests of SCS panels investigated the influence of concrete infill (they tested some panels with no concrete), concrete thickness, and steel plate thickness for a variety of charge weights at a constant stand-off distance. Liew & Wang (2011) conducted blast tests on a unique configuration of SCS and a type of panel they called cellular stiffened plate (SP). The SCS panels had j-hooks in place of headed stud anchors and tie bars. The SP configuration connected steel faceplates with internal steel stiffeners. They tested panels with different steel plate thicknesses subjected to blasts of the same charge weight and stand-off distance. They concluded that increased steel faceplate thickness improved blast resistance of the structure and the type of concrete infill influenced the type of failure experienced by the panel. Hulton (1995) provided a qualitative summary of blast tests conducted by the United Kingdom Defence Research Agency of steel-backed reinforced concrete - some with steel plates on the back-face alone and others with steel plates on both front- and back-faces. The author concluded that panels with plates on both sides performed better than those with only back-plates but that front-plates were inefficient because of fragment damage or buckling.

Hulton & Gough (1999) discussed development of Bi-Steel™, a proprietary product of British Steel PLC (now Tata Steel). The authors described various configurations of SCS composite sections and explained how the Bi-Steel™ design overcame weaknesses of each. Bi-Steel™ walls consist of two steel faceplates connected by friction welded transverse bar connectors. These modular sections could be cast with concrete in the factory and shipped to their intended location or set in place, welded to each other, and filled with concrete on site. The authors reported general behavior of the panels in blast tests but provided no details on test specimens, blast loads applied, or observed damage. Coyle & Cormie (2009) described blast resistant design of SCS composite sections, addressed similarities and differences between RC and SCS, and discussed computation of strength and stiffness. They focused on Bi-Steel™ and the information was not general enough to be of use for other configurations of SC walls.

Of the different configurations that have been tested, Bi-Steel™ is most similar to the general SC system described in this paper but is proprietary and has key differences from SC structures designed in accordance with AISC N690s1 Appendix N9. For example, Bi-Steel™ does not include headed stud anchors and its flexural reinforcement is often larger than the 5% maximum permitted by N690s1 N9.

EXPERIMENTAL PERFORMANCE OF SC WALLS SUBJECTED TO BLAST LOADS

An experimental investigation by Bruhl (2015) of one-third scale SC wall sections subjected to blast loads studied the influence of design and blast load parameters on SC wall performance (see Table 1).

Table 1 Experimentally Varied Parameters

Design Parameter	Range Considered
Steel Plate Strength	A1011 HLSA Grade 50 to 80
Steel Plate Thickness, t_p	14 to 12 Gage
Flexural Reinforcement Ratio, ρ	3.5% to 5.6%
Shear Reinforcement Ratio, ρ_t	0.37% to 1.23%
Shear Reinforcement Spacing, S	$t_{sc}/2$ to t_{sc}
Peak Reflected Pressure, p_r	18.9 to 61.6 psi
Peak Reflected Impulse, i_r	260 to 1110 psi·msec

Specimen Design

Specimens were designed in accordance with AISC N690s1 Appendix N9 and current blast resistant design methods for RC explained in UFC 3-340-02 Chapter 4, to account for dynamic shear demand. Because the specimens were one-third scale and faceplate strength was intentionally varied, they were not in accordance with every aspect of N690s1 N9:

- The smallest plate thickness permitted is 0.25-in; these specimens used 12 and 14 gage sheet (nominally 0.105-in or 0.075-in respectively),
- Grade 80 steel is not permitted, and
- The maximum permitted flexural reinforcement ratio of 5.0% was exceeded for three specimens; actual plate thickness of the 12 gage Grade 50 sheet was slightly larger than nominal.

As shown in Figure 2, each specimen had identical global dimensions: 4-in total thickness, t_{sc}; 11-in width, b; 64-in total length; and 52-in unsupported length, L. A1011 HSLA hot-rolled steel sheets were used for top and bottom faceplates. Steel sheet grade and gage varied between specimens. All specimens were cast from the same concrete batch. Concrete aggregate was pea gravel with a maximum diameter of 0.375-in. Day-of-test concrete cylinder strengths, f'_c, were between 6.2 and 6.5-ksi. Threaded rods provided transverse shear reinforcement. Diameter of the rods, d_t, varied from 0.138-in to 5/16-in. Holes were drilled in the faceplates 1/32-in larger than the tie bar diameter. Tie bars extended through the holes and were secured with hex nuts on both sides of the faceplate. All specimens included 0.25-in diameter (d_s) 1.125-in long, headed shear stud anchors spaced, s, at 2-in on-center.

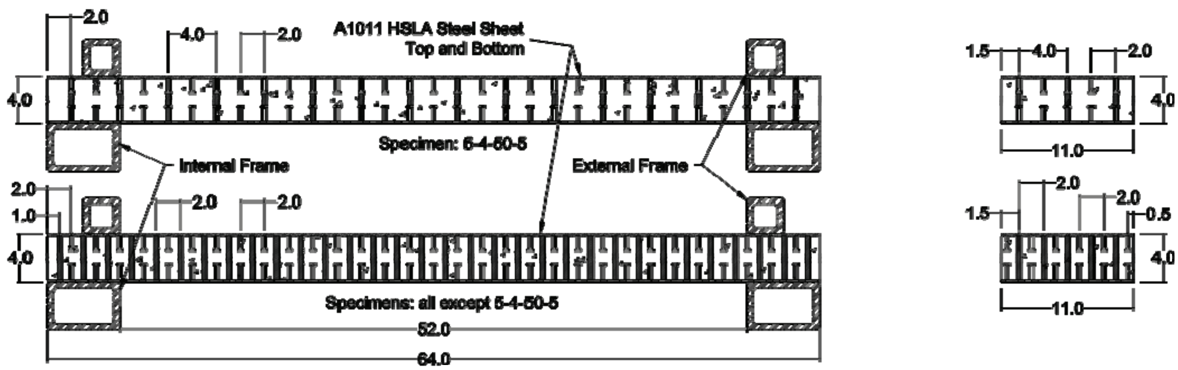

Figure 2 Blast Specimen Design Schematic (units are inches)

Test Setup

The BLS, shown in Figure 3, is a compressed-gas-driven shock tube which can be tuned to simulate far-field blast waveforms. It consists of: (i) a driver and pressure vessel which is pressurized with a combination of helium and air, (ii) vented cone and transition components which shape the pressure wave, and (iii) a target vessel to support the tested specimens and contain any debris (Johnson 2013). The BLS permits extensive instrumentation of specimens and there is no fireball or debris cloud from an explosion to obscure video recordings of the tests.

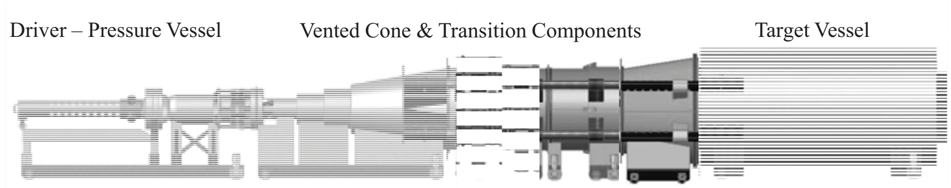

Figure 3 Schematic of USACE-ERDC BLS (after C. F. Johnson (2013))

Three specimens were tested simultaneously during each of four setups (see Figure 4). The frame installed in the target vessel provided approximately simple supports of the specimens. In each of the first two setups, two shots were conducted. The first shot was designed to result in elastic response of the specimens and the second, larger pressure, shot was expected to result in plastic deformation. Each of the last two setups subjected the specimens to the larger pressure shot.

The layout and type of sensors was identical for each of the four tests (Figure 4). Eight pressure gauges around the perimeter of the frame recorded the pressure-time history. A ninth pressure gauge recorded the pressure inside the target vessel. Potentiometers recorded mid-span deflection of each. As an alternate measure, mid-span deflection was calculated from mid-span accelerometer data. Cable-extension transducers recorded deflection 8.75-in away from mid-span. Strains were measured at mid-span on the compression (blast) face and the quarter-points on the tension (non-blast) face of each specimen.

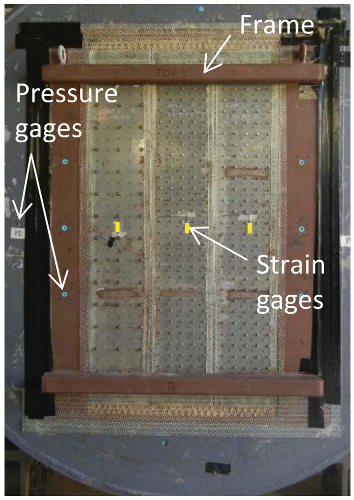

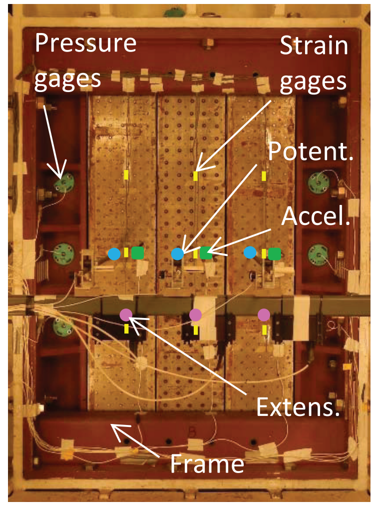

(a) Blast Face (b) Non-Blast Face

Figure 4 Specimen Setup in BLS (Pre-test Photos) With Sensor Layout

Three high-speed video cameras documented the specimen responses (left, right, and rear angles) and pre- and post-test still photos were taken. Residual displacements were measured prior to removing specimens from the target vessel. After each test was complete, the three specimens were removed from the frame and cracks along the sides were marked and photographed.

Experimental Results

For brevity, representative results from one specimen from the second setup are discussed in this paper. Complete experimental results from all sensors for all six shots are provided by Bruhl (2015). This representative specimen was comprised of 12 gage Gr50 A1011 HSLA steel sheets, 0.25-in tie bars spaced at 2-in on-center, and 6.3-ksi concrete. Measured stress-strain curves of the steel components are shown in Figure 5. Included on this figure are idealizations of the measured curves which were used as input for numerical models.

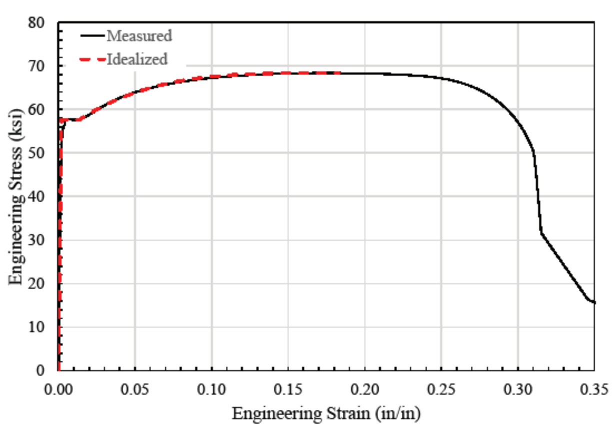

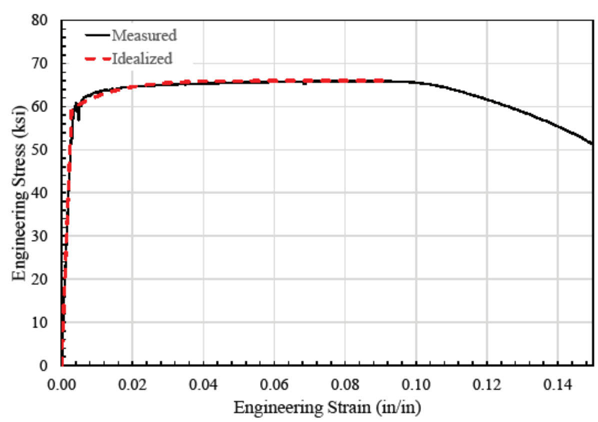

(a) 12 gage, Gr50 A1011 HSLA Sheet (b) Tie Bars

Figure 5 Measured Steel Stress-Strain Curves

This specimen was subjected to two pressure loads. Representative pressure time-histories for each shot are provided in Figure 6. Overlaid on the measured data in this figure is an idealized exponential decay function which served as input for numerical models. The idealization modified the Friedlander waveform (Baker et al., 1983) to include a finite rise time to peak pressure, p_r. The average maximum measured pressure from the eight pressure gages on the face of the target vessel for each of the two shots is provided with the average peak impulse in the captions of Figure 6.

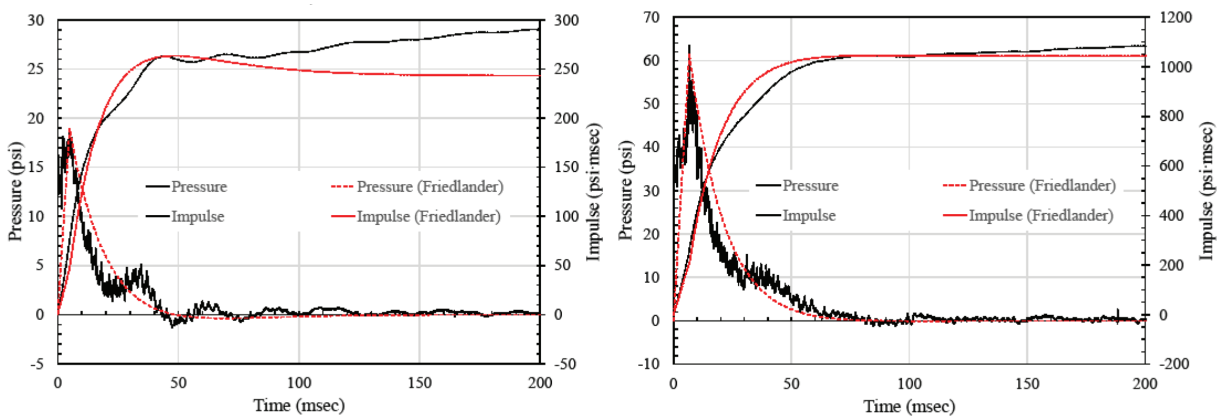

(a) Shot 3 (p_r = 18.9-psi; i_r = 260psi·ms) (b) Shot 4 (p_r = 61.6-psi; i_r = 950psi·ms)

Figure 6 Measured and Idealized Pressure Time-History and Calculated Impulse

The displacement time history for the representative specimen for both shots is provided in Figure 7. The measured value from the extensometer was at a location away from mid-span and expected to be less than mid-span displacement. Because of numerical errors, only the first peak displacement value calculated from accelerometer data is valuable but the potentiometer and extensometer transient displacement data is valuable. Despite being post-tensioned, the frame displaced as a rigid body during each test and maximum displacement of the frame was determined from analysis of high-speed video recordings. Corrected values accounting for frame displacement are provided in the captions of Figure 7 for maximum and residual displacement, X_M and X_r respectively.

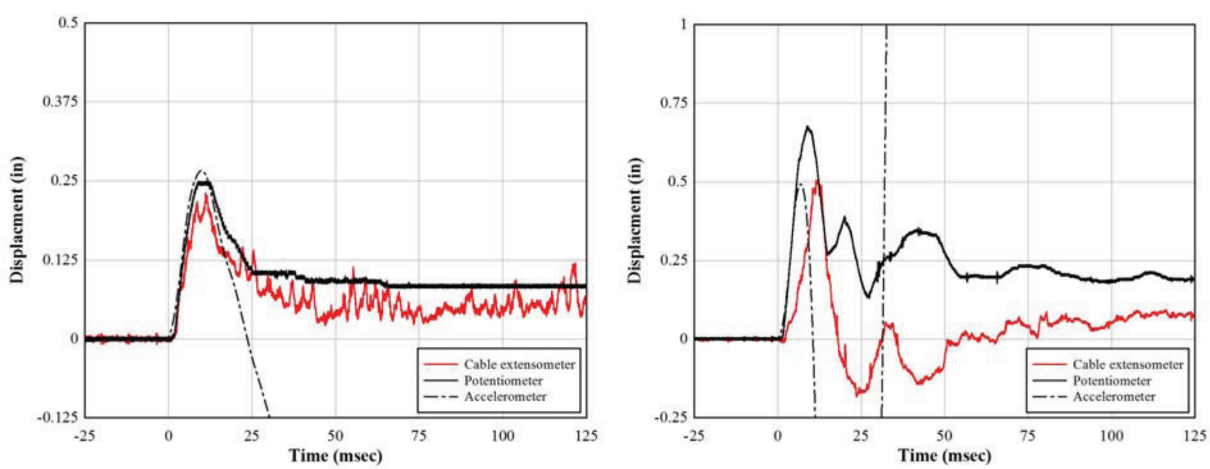

(a) Shot 3 (X_M = 0.10-in; X_r = 0.08-in) (b) Shot 4 (X_M = 0.53-in; X_r = 0.24-in)

Figure 7 Measured Displacement Time-History

Measured strains of the specimen for the two shots are shown in Figure 8. The black lines are the strains at the quarter points of the non-blast (tension) faceplate and the red line is the strain at mid-span of the blast (compression) faceplate. The strains during Shot 3 were below yield (~2000-με) demonstrating that the specimen responded elastically. Results from Shot 4 show that the larger load resulted in plastic deformation – maximum tensile strain at mid-span was beyond yield. The peak compressive strain of the blast face plate was also close to yield. There was no evidence of concrete crushing.

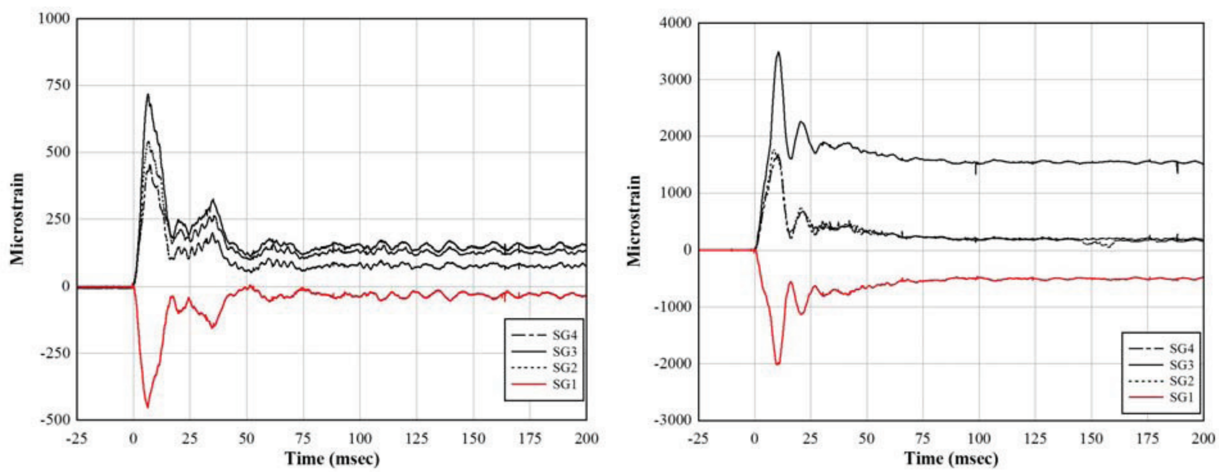

(a) Shot 3 (X_M = 0.10-in; X_r = 0.08-in) (b) Shot 4 (X_M = 0.53-in; X_r = 0.24-in)

Figure 8 Measured Strain Time-History

NUMERICAL MODELS

Two numerical models were benchmarked to the experimental results: (1) a lumped mass SDOF model and (2) a detailed non-linear FE model. For brevity, a summary of each modelling method is provided below. Detailed information about input parameters for both models is provided by Bruhl (2015).

SDOF Model

An idealized lumped mass SDOF model is a common tool in blast resistant design of structural elements (ASCE 59-11; Smilowitz, et al., 2010; UFC 3-340-02). The SDOF model for this analysis included:

- The idealized pressure time-history shown in Figure 6,
- An idealized experimentally validated bi-linear static resistance function computed from section geometric and material properties, including dynamic increase factors (DIF) (Bruhl 2015), and
- The mass of the unsupported length estimated from the measured mass of the entire specimen.

The effect of damping is often neglected in analysis supporting blast resistant design. For comparison purposes, the model was analyzed with 0% damping and 5% damping. The equation of motion for the SDOF model was solved numerically using the constant acceleration method.

FE Model

A detailed non-linear FE model was analyzed using LS-DYNA (Hallquist 2006). The model, shown in Figure 9, consisted of solid elements for the concrete infill, steel faceplates, and supports and beam elements for stud anchors and tie bars. The concrete core was modelled using the Winfrith concrete model. When the strain rate effects were included in the Winfrith model inaccurate results were obtained.

Instead, DIFs for concrete compressive strength, tensile strength, and fracture energy were applied directly to input values. Steel properties were input using the idealized piecewise curves from Figure 5. DIFs were applied to steel yield strength. Studs were connected to faceplates using zero-length connector elements which accounted for load-slip behavior (Zhang et al., 2014).

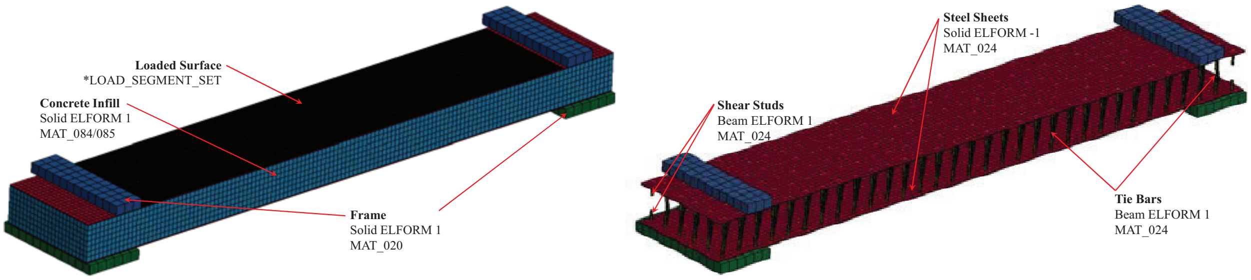

(a) Specimen in Frame (b) Internal Components

Figure 9 FE Model Overview

Comparison of Results

A comparison of experimentally measured displacements to those computed from the numerical methods is provided in Table 2. The SDOF model with 0% damping provided a conservative estimate of maximum response of this specimen for both shots and the FE model was nearly exact for this specific case. Including 5% damping in the SDOF analysis had small influence on the estimated response in the elastic region but decreased the maximum displacement for the larger shot by 17%.

Table 2 Representative Blast Tests Results

				SDOF					
		Experiment		0% Damping		5% Damping		FE	
Setup	**Shot**	X_M **(in)**	X_r **(in)**	X_M **(in)**	X_r **(in)**	X_M **(in)**	X_r **(in)**	X_M **(in)**	X_r **(in)**
2	3	0.10	0.08	0.15	0.00	0.14	0.00	0.10	0.00
	4	0.53	0.24	0.56	0.25	0.46	0.10	0.53	0.16

The displacement time-history from the SDOF model with 0% and 5% damping considered and the FE model are shown in Figure 10. A direct comparison to the experimental values in Figure 7 is difficult because the measured data included the rigid body displacement but the shape of the transient response is most similar between the FE model results and the experimental response.

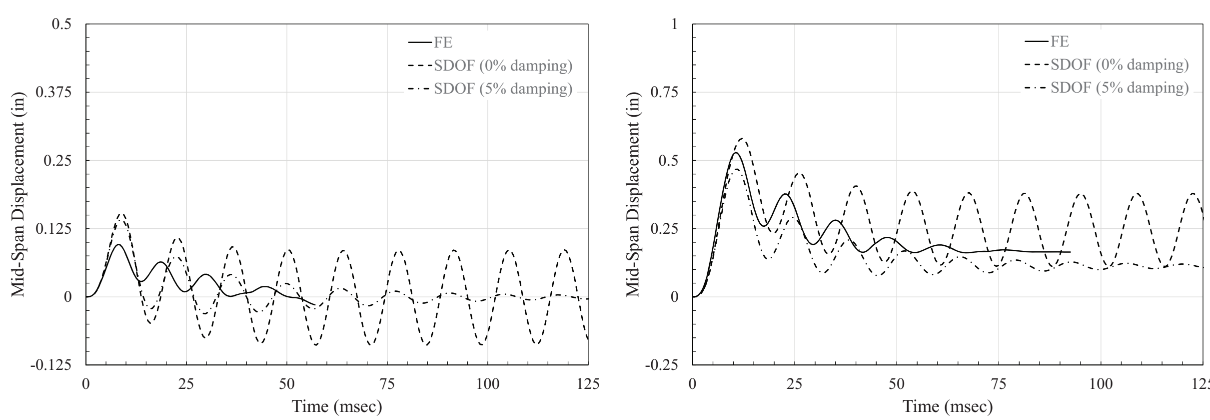

(a) Shot 3 (b) Shot 4

Figure 10 Numerical Analysis Displacement Time-History

The strain time-history from the FE model for both shots of this representative specimen are shown in Figure 11. Neither analysis was run for the same length of time as shown in the experimental data but the horizontal scale for these figures was the same as Figure 8 for ease of comparison. Strains for the elastic response were similar between the FE model and experimental results. For the plastic response, the FE model predicted larger tensile strains and smaller compressive strains at mid-span than experimentally observed indicating the neutral axis was closer to the top of the cross section in the numerical model than in the experiment.

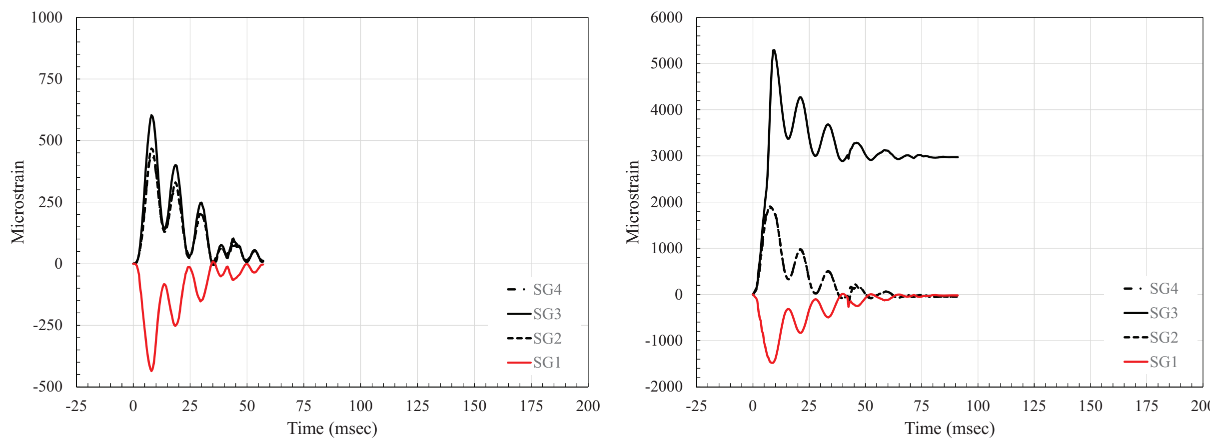

Figure 11 Numerical Analysis Strain Time-History

CONCLUSIONS

This paper described a recent experimental investigation of structural performance of simply supported one-way SC walls subjected to short duration uniform pressure loads using the USACE-ERDC BLS. The specimens tested were designed as flexure-controlled in accordance with provisions for SC walls in safety related nuclear facilities (AISC N690s1 N9) and accounted for dynamic shear demands.

Detailed results were provided for a representative specimen subjected to two loads: a lower pressure designed to result in elastic response and a higher pressure designed to yield the section. Two numerical modelling methods were presented and, for the representative specimen, the SDOF and non-linear FE analyses provided good estimates of maximum and residual displacement. The SDOF model was generally conservative when 0% damping was considered and underestimated the response when 5% damping was included in the solution.

ACKNOWLEDGEMENTS

The authors gratefully acknowledge the assistance of Dr. Carol Johnson, USACE-ERDC, and her technical staff for their efforts during planning and execution of this experimental program. Thanks also to Mr. Thomas Bradt and Mr. Graham Marshall for assistance in fabricating, shipping, and testing the specimens. This research was funded by the U.S. Department of Energy (SL-14ID020104) and the American Institute of Steel Construction.

REFERENCES

American Institute of Steel Construction. (2012). "Specification for Safety-Related Steel Structures for Nuclear Facilities (ANSI/AISC N690-12)." American Institute of Steel Construction, Chicago, IL.

American Institute of Steel Construction. (2014). "Specification for Safety-Related Steel Structures for Nuclear Facilities Supplement No. 1 (AISC N690s1) PUBLIC REVIEW DRAFT DATED 5-1-14." American Institute of Steel Construction, Chicago, IL.

American Society of Civil Engineers. (2011). "Blast Protection of Buildings (ASCE/SEI 59-11)." American Society of Civil Engineers, Reston, VA.

Baker, W. E., Cox, P. A., Westine, P. S., Kulesz, J. J., and Strehlow, R. A. (1983). *Explosion Hazards and Evaluation (Fundamental Studies in Engineering 5)*. Elsevier Science, New York, NY.

Bruhl, J. C. (2015). "Behavior and Design of Steel-Plate Composite (SC) Walls for Blast Loads." Doctoral dissertation. Purdue University.

Bruhl, J. C., Johnson, W. H., Reigles, D. G., Kim, J. M., Li, J., and Varma, A. H. (2015a). "Impact Assessment of SC Walls Using Idealized SDOF and TDOF Models." *Structures Congress 2015*, Portland, OR.

Bruhl, J. C., Varma, A. H., and Johnson, W. H. (2015b). "Design of composite SC walls to prevent perforation from missile impact." *Intl J Impact Eng*, 75, 75-87.

Bruhl, J. C., Varma, A. H., and Kim, J. M. (2015c). "Static Resistance Function for SC Walls Subject to Impactive Loads." *Nuc Eng Des*. In press.

Coyle, N., and Cormie, D. (2009). "Design of elements in steel-concrete-steel composite materials." *Blast effects on buildings*, D. Cormie, G. Mays, and P. Smith, eds., Thomas Telford, London, UK, 154-176.

Grisaro, H., and Dancygier, A. (2014). "Assessment of the perforation limit of a composite RC barrier with a rear steel liner to impact of a non-deforming projectile." *Intl J Impact Eng*, 64, 122-136.

Hallquist, J. (2006). *LS-DYNA theory manual. Livermore Software Technology Corporation*, Livermore Technology Software Corporation, Livermore, CA.

Heng, L., Kennedy, L. J., and Mays, G. C. (1995). "Blast Resistance of Fully Enclosed Steel-Concrete-Steel Standwich Panels." *7th International Symposium on Interaction of the Effects of Munitions with Structures*, Mannheim, Germany, 189-197.

Hulton, F. G. (1995). "The Behavior of Steel-backed Reinforced Concrete Panels under Explosive Attack." *7th International Symposium on Interaction of the Effects of Munitions with Structures*, Mannheim, Germany, 111-116.

Hulton, F. G., and Gough, M. S. (1999). "The development of steel-plate/reinforced concrete composite panels to resist explosive attack." *9th International Symposium on Interaction of the Effects of Munitions with Structures*, Berlin-Straussberg, Germany, 63-69.

Johnson, C. F. (2013). "Concrete Masonry Wall Retrofit Systems for Blast Protection." Doctoral dissertation. Texas A&M University.

Johnson, W., Bruhl, J., Reigles, D., Li, J., and Varma, A. (2014). "Missile Impact on SC Walls: Global Response." *Structures Congress 2014*, 1403-1414.

Lan, S., Lok, T.-S., and Heng, L. (2005). "Composite structural panels subjected to explosive loading." *Constr Build Mater*, 19(5), 387-395.

Liew, J. Y. R., and Wang, T. Y. (2011). "Novel Steel-Concrete-Steel Sandwich Composite Plates Subject to Impact and Blast Load." *Adv Struct Eng*, 14(4), 673-688.

Smilowitz, R., and Tennant, D. (2010). "Structural Systems Design." *Handbook for Blast-Resistant Design of Buildings*, D. O. Dusenberry, ed., John Wiley & Sons, Inc, Hoboken, NJ, 241-262.

U.S. Department of Defense. (2008). "Structures to Resist the Effects of Accidental Explosions (UFC 3-340-02)." U.S. Department of Defense, Washington, D.C.

Varma, A. H., Malushte, S. R., Sener, K. C., and Lai, Z. (2014). "Steel-plate composite (SC) walls for safety related nuclear facilities: Design for in-plane forces and out-of-plane moments." *Nuc Eng Des*, 269, 240-249.

Zhang, K., Varma, A. H., Malushte, S. R., and Gallocher, S. (2014). "Effect of shear connectors on local buckling and composite action in steel concrete composite walls." *Nuc Eng Des*, 269, 231-239.